ISSN 1062-8738, Bulletin of the Russian Academy of Sciences: Physics, 2018, Vol. 82, No. 6, pp. 685–690. © Allerton Press, Inc., 2018.
Original Russian Text © E.V. Vladimirova, I.D. Dashkov, B.S. Ishkhanov, T.Yu. Tretyakova, 2018, published in Izvestiya Rossiiskoi Akademii Nauk, Seriya Fizicheskaya, 2018, Vol. 82, No. 6.

Mass Ratios and Proton Pairing for Isotones with $N = 20$, 50, and 82

E. V. Vladimirova[a, b], I. D. Dashkov[a], B. S. Ishkhanov[a, b], and T. Yu. Tretyakova[b, *]

[a]*Faculty of Physics, Moscow State University, Moscow, 119991 Russia*
[b]*Skobeltsyn Institute of Nuclear Physics, Moscow State University, Moscow, 119991 Russia*
**e-mail: tretyakova@simp.msu.ru*

Abstract—Different estimates of the even–odd effect for the nuclear mass surface are discussed. The proton-number dependence of the energy gap is derived from the measured masses of the $N = 20$, 50, and 82 isotones with closed neutron shells. Its interrelation with the properties of external proton shells is demonstrated, and the effects of proton pairing are considered along with the microscopic nuclear structure.

DOI: 10.3103/S1062873818060345

INTRODUCTION

The formulation of the nuclear shell model [1, 2] was a landmark achievement of theoretical nuclear physics. This nuclear scheme was originally modeled after that of atomic electron shells. Its viability was not at all obvious, due to the considerable differences between constituent nucleons and atomic electrons. Atomic electrons are affected by the strong Coulomb field of nucleons, and inter-electron interaction can be considered as a correction to the nucleus Coulomb potential (a more important effect is the electron screening of the Coulomb field). At the same time, constituent nucleons are affected by the common self-consistent nuclear field resulting from nucleon–nucleon interaction and reflecting its properties. The common nuclear potential varies from one isotope to another.

Apart from the common self-consistent potential, we must also consider so-called residual interaction, which can strongly affect the properties of a nucleon system despite its relative smallness. In the first approximation, residual interaction is reduced to the so-called pairing force as short-range interaction that effectively raises the nucleon-pair bonding energy when nucleon spins add up to a total angular momentum of $J = 0$. Many experimental observations (e.g., the $J^\pi = 0^+$ spin-parity values of all even–even nuclei and the enhanced stability displayed by even–even isotopes) can be explained by the pairing of identical nucleons [3, 4].

EVEN–ODD EFFECT OF A NUCLEAR MASS SURFACE

Due to the enhanced stability of even–even nuclei, a nuclear mass surface (showing the Z- and N-dependences of the nuclear mass) splits into three components corresponding to even–even, odd–odd, and intermediate odd–A nuclei. As demonstrated by systematic studies of nuclear bonding energies $B(A)$, those for even–even nuclei obey the rule

$$B(A) > \frac{1}{2}\big(B(A+1) + B(A-1)\big). \qquad (1)$$

This is referred to as the effect of even–odd staggering (EOS) used to estimate pairing forces between identical nucleons. Pairing energies for identical nucleons are derived using mass relations involving the bonding energies of neighboring isotones or isotopes for proton and neutron pairs, respectively [5–9]. The basic relations for the EOS effect involving the bonding energies of three or four neighboring nuclei are written as [5]

$$\Delta_p^{(3)}(Z) = \frac{(-1)^Z}{2}\big(S_p(Z) - S_p(Z+1)\big), \qquad (2)$$

$$\Delta_p^{(4)}(Z) = \frac{(-1)^Z}{2} \times \big(2S_p(Z) - S_p(Z+1) - S_p(Z-1)\big),$$

where neutron number N is fixed and $S_p(Z) = B(Z) - B(Z-1)$ is the energy of proton separation for an (N, Z) nucleus. The neutron EOS effect is achieved by substituting N for Z in Eqs. (2) and fixing proton number Z.

It follows from Eqs. (2) that $\Delta_p^{(4)}(Z)$ is the mean value of $\Delta_p^{(3)}(Z)$ and $\Delta_p^{(3)}(Z-1)$. Analogous equations based on the bonding energies of five and six neighboring nuclei essentially result from further averaging. Increasing the number of neighboring nuclei has no appreciable effect on the final results from EOS calcu-

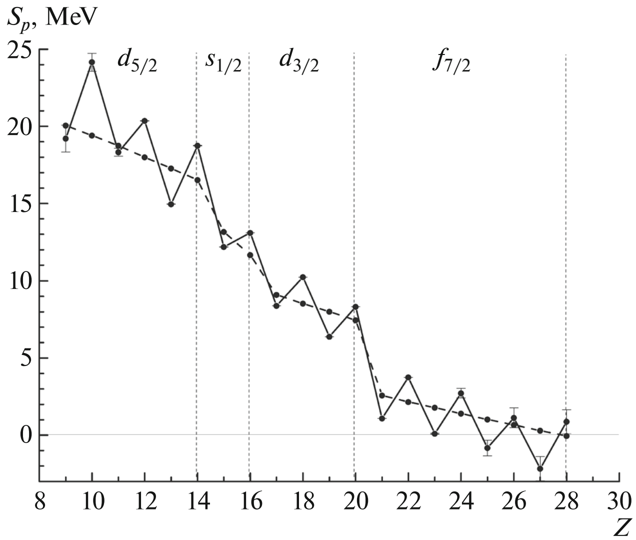

Fig. 1. Energy $S_p(Z)$ of proton separation for $N = 20$ isotones, derived from the data in [12] on nuclear masses (solid line) and calculated using the SHF formalism (dashed line).

lations, but the concurrent expansion of the range of experimental data in going beyond the region of stability could require the use of nucleus bonding energies whose values are known less precisely. We must also consider that subshells with low orbital momenta of $l = 0$, 1, and 2 are populated by small numbers of particles, so averaging over a broad Z interval smooths out shell effects.

Neutron pairing was analyzed in [10], where the relative contributions from nucleon pairing and other many-particle phenomena to the EOS effect were discussed in detail. It was shown in particular that for an even-N nucleus, the best estimate of neutron pairing is given by $\Delta_n^{(3)}(N-1)$ for odd numbers of neutrons. This conclusion is consistent with the definition of the pairing energy of two identical nucleons as the difference between the energy of nucleon-pair separation and the doubled energy of nucleon separation for nuclei with mass numbers of A and $A - 1$, respectively [11]. The analogous equation for a proton pair has the form

$$\begin{aligned} \Delta_{pp}(Z) &= S_{2p}(Z) - 2S_p(Z-1) \\ &= S_p(Z) - S_p(Z-1) = 2\Delta_p^{(3)}(Z-1), \end{aligned} \tag{3}$$

where $S_{2p}(Z) = B(Z) - B(Z-2)$ is the energy of two-proton separation for an (N, Z) nucleus. In this approach, an (N, Z) nucleus is visualized as a combination of an $(N, Z-2)$ core nucleus and two external nucleons in its field. The potential of the latter nucleus is assumed to remain the same upon adding or removing external nucleons.

ENERGY OF NUCLEON SEPARATION

By definition, proton-pairing energy $\Delta_{pp}(Z)$ (3) corresponds to doubled even–odd effect $\Delta_p^{(3)}(Z-1)$. The proton-pairing energy is thus expressed below as

$$\Delta_{pp}^{(3)}(Z) = 2\Delta_p^{(3)}(Z), \tag{4}$$

$$\Delta_{pp}^{(4)}(Z) = 2\Delta_p^{(4)}(Z).$$

Since Eqs. (2) and (3) depend on the energy of nucleon separation, let us consider the Z-dependence of the proton separation energy for isotone nuclei with $N =$ const. The one for $N = 20$ has a pronounced sawtooth shape that reflects the pairing effect (see Fig. 1). The steep variations where $Z = 14$, 16, and 20 correspond to transitions between different subshells.

In the seniority model, the energy n of external nucleons in core–nucleus field $B(j^n)$ is written as [13, 14]

$$\begin{aligned} B(j^n) &= B_{\text{core}}(n=0) + n\varepsilon_j \\ &+ \frac{n(n-1)}{2}\alpha - \frac{1}{2}\left[n - \frac{1-(-1)^n}{2}\right]\beta. \end{aligned} \tag{5}$$

The corresponding one-nucleon energy of separation,

$$\begin{aligned} S(N) &= B(j^n) - B(j^{n-1}) \\ &= \varepsilon_j + (n-1) + \frac{1+(-1)^n}{2}\beta, \end{aligned} \tag{6}$$

includes the term ε_j arising from the nucleon kinetic energy for the j-th shell and the nucleon–core interaction, a term proportional to β that corresponds to the pairing effect, and a term proportional to α that describing the general slope of the $S_p(Z)$ dependence. Coefficients α and β can be expressed through the matrix elements of two-body interaction between valence nucleons; i.e., pairing interaction contributes to the common self-consistent potential, along with making the $S_p(Z)$ dependence sawtooth-shaped. The jump at $Z = 20$ is due to difference $\varepsilon_{j1} - \varepsilon_{j2}$ between the ε values for the j_1 and j_2 subshells.

The $S_p(Z)$ values for $N = 20$ isotones, calculated in the Hartree–Fock approximation with Skyrme interaction (SHF) using SLy230b parametrization [15], which adequately reproduces the nuclear binding energies over a broad mass-number interval, are also shown in Fig. 1 for comparison. For the above isotone groups, the energies of proton separation calculated for even–even nuclei agree with those obtained using nuclear masses within 3 MeV. Note that in order to determine the role of other microscopic effects, nucleon pairing was not included in our SHF calculations. The calculated $S_p(Z)$ dependence thus lacks the characteristic sawtooth shape but reproduces the general slope reflecting the variation of the self-consistent field with increasing Z and the characteristic jumps corresponding to subshell closures.

ENERGY OF NUCLEON-PAIRING INTERACTION

The $S_p(Z)$ dependence within a given subshell means that for even Z values, Eq. (3) always yields a smaller value of the pairing energy than Eq. (4):

$$\Delta_{pp}(Z) < \Delta_{pp}^{(3)}(Z). \quad (7)$$

This result agrees with predictions from the simplest seniority model, in which

$$\Delta_{pp}^{(3)}(Z) = G\Omega + G, \quad (8)$$

$$\Delta_{pp}(Z) = G\Omega,$$

and other estimates based on four or more $B(A)$ values of neighboring nuclei are identical and equal to the mean value of the former two [16]:

$$\Delta_{pp}^{(4)}(Z) = G\Omega + \frac{1}{2}G. \quad (9)$$

Here, G is the nucleon pairing parameter for a shell with total angular momentum j ($2\Omega = 2j + 1$).

The $\Delta_{pp}(Z)$ estimates obtained with formulas (3) and (4) are shown in Fig. 2 for $N = 20$ isotones with Z between 10 and 28. Note that $\Delta_{pp}(Z)$ and $\Delta_{pp}^{(3)}(Z)$ coincide upon shifting Z by one unit and $\Delta_{pp}^{(4)}(Z)$ equals the mean value of the former two. In the $S_p(Z)$ dependence, the jump at $Z = 20$ marks the closure of the $1d2s$ shell and the subsequent filling of the $f_{7/2}$ shell. The corresponding $\Delta_{pp}^{(3)}(Z)$ and $\Delta_{pp}(Z)$ jumps occur at even and odd Z values of $Z = 20$ and 21, respectively. The $\Delta_{pp}^{(3)}(Z)$ dependence for even–even nuclei thus fluctuates considerably in the regions of magic numbers, while $\Delta_{pp}(Z)$ for even Z is more regular and always lies below $\Delta_{pp}^{(3)}(Z)$.

It is interesting to trace the Z-dependence of the difference between $\Delta_{pp}(Z)$ and $\Delta_{pp}^{(3)}(Z)$, which is equal to pairing parameter G in the simplest seniority model. Deriving

$$\delta e(Z) = (-1)^Z \left(\Delta_{pp}^{(3)}(Z) - \Delta_{pp}(Z)\right) \quad (10)$$

from Eqs. (2)–(4), we obtain $\delta e(Z) = S_p(Z - 1) - S_p(Z + 1)$. The form of the $S_p(Z)$ dependence shown in Fig. 1 means quantity δe is not affected by nucleon pairing and can be viewed as a correction arising from core polarization and/or three-body interaction [17].

RESULTS FOR MAGIC NUCLEI

Proton-pairing energy $\Delta_{pp}^{(4)}(Z)$ for isotones with $N = 20$ and neutron-pairing energy $\Delta_{nn}^{(4)}(N)$ for Ca isotopes ($Z = 20$) are shown in Fig. 3a. In contrast to $\Delta_{pp}(Z)$ and $\Delta_{pp}^{(3)}(Z)$, this estimate of pairing energy

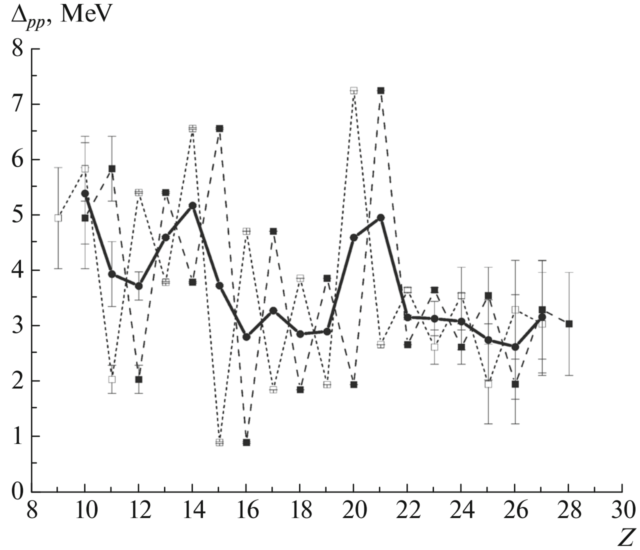

Fig. 2. Estimates of the proton pairing energy for the isotones with $N = 20$ and $Z = 10$–28, derived from the data in [12]: (●) $\Delta_{pp}^{(4)}(Z)$, (■) $\Delta_{pp}(Z)$, and (□) $\Delta_{pp}^{(3)}(Z)$.

accurately describes the observed mass splittings in the multiplets of excited states in nuclear spectra that arise from the pairing of external nucleons [16]. In estimating microscopic effects, the $\Delta_{pp}^{(4)}(Z)$ and $\Delta_{nn}^{(4)}(N)$ values derived from nuclear masses are compared to those calculated using the SHF approach with Sly230b parametrization (the dashed line in Fig. 3a). For the Z or N values in the middle of a subshell, SHF calculations without nucleon pairing yield $\Delta^{(4)}$ values below 50 keV that are comparable to or less than the uncertainties on the $\Delta^{(4)}$ values derived from the measured bonding energies. The above dependences clearly reflect the process of subshell filling, as the plateaus and peaks correspond to subshell internal regions and closures, repectively. Subshell closures within the shell model, represented by the vertical dotted lines in Fig. 3a, are seen to correspond to the maxima of the $\Delta_{nn}^{(4)}(N)$ and $\Delta_{pp}^{(4)}(Z)$ dependences. The most pronounced peak corresponding to the $1d2s$ shell closure is observed at $N = Z = 20$ (^{40}Ca), where the energy of symmetry also plays an important role.

For the Z or N values inside a subshell, the $\Delta^{(4)}$ value derived in the SHF approximation is virtually independent of the interaction parameters as a consequence of the characteristic form of the predicted SHF dependence $S_p(Z)$ with no nucleon pairing (see Fig. 1). On the other hand, the heights of the peaks corresponding to subshell closures are strongly affected by how the Skyrme forces are parametrized. The data of Fig. 3b that show the differences between the experimental and predicted SHF dependences for $\Delta_{nn}^{(4)}(N)$

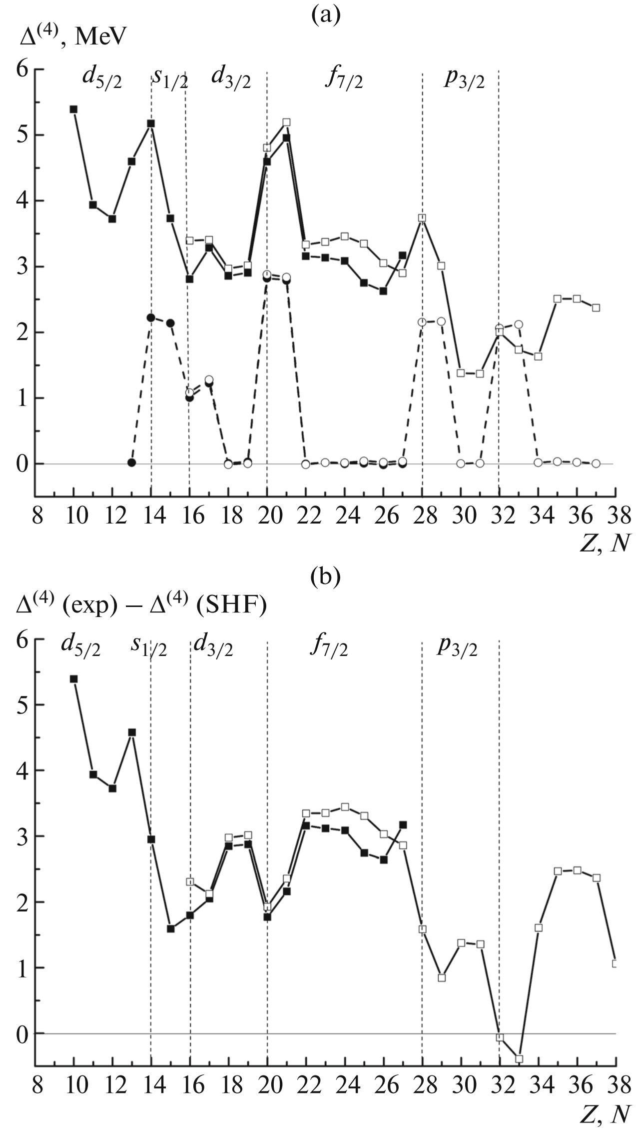

Fig. 3. (a) (▪) Proton pairing energy $\Delta^{(4)}_{pp}(Z)$ for the isotones with $N = 20$ and $Z = 10–28$ and (■) neutron pairing energy $\Delta^{(4)}_{nn}(N)$ for Ca isotopes with N = 16–38, (□) derived from the nuclear-mass data in [12] and calculated using the SHF formalism without pairing (dashed line). (b) Differences between the experimental and SHF-computed values for (■) $\Delta^{(4)}_{pp}(Z)$ and (□) $\Delta^{(4)}_{nn}(N)$.

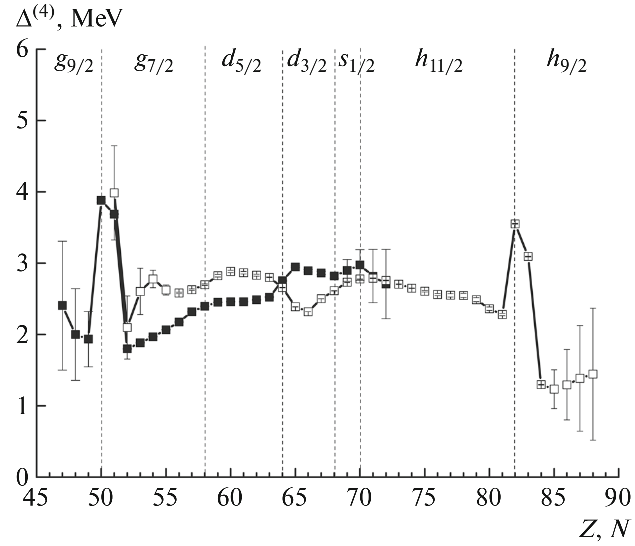

Fig. 4. (■) Proton pairing energy $\Delta^{(4)}_{pp}(Z)$ for $N = 82$ isotones and (□) neutron pairing energy for Sn isotopes with $Z = 50$, derived from nuclear-mass data in [12].

and $\Delta^{(4)}_{pp}(Z)$ should therefore be considered qualitative, but they adequately reproduce the characteristic variation of the pairing energy of identical nucleons depending on their number. It grows along with subshell occupancy, and then falls as we approach complete filling.

Chains of isotones with $N = 20$ and isotopes with $Z = 20$ offer a unique opportunity to compare proton and neutron pairings. Both Coulomb interaction and neutron excess grow along with A. The higher A, the greater the differences between the proton and neutron self-consistent fields, and between the residual proton and neutron pairing interactions. Neutron and proton pairing energies $\Delta^{(4)}_{nn}(N)$ and $\Delta^{(4)}_{pp}(Z)$ are shown in Fig. 4 for $Z = 50$ isotopes and $N = 82$ isotones, respectively. In the one-particle model, shell filling proceeds with considerable mixing between the subshells for nuclei with $N, Z > 50$. As a result, the $\Delta^{(4)}_{nn}(N)$ and $\Delta^{(4)}_{pp}(Z)$ dependences are relatively smooth and show no pronounced kinks when subshells are filled. The small kink at $N = 66$ in the $\Delta^{(4)}_{nn}(N)$ dependence indicates subshell groups ($d_{5/2}$, $g_{7/2}$) and ($s_{1/2}$, $d_{3/2}$, $h_{11/2}$) are separated by an energy gap. The abrupt jump of $\Delta^{(4)}_{nn}(N)$ at $N = 82$ marks the transition to the next shell, and the drop in pairing energy is explained by the reduced number of j projections for external shells [20]: 16 and 8 projections for the ($d_{3/2}$, $h_{11/2}$) subshell and the more isolated $f_{7/2}$ subshell, respectively. The $\Delta^{(4)}_{pp}(Z)$ and $\Delta^{(4)}_{nn}(N)$ dependences differ both quantitatively and qualitatively, indicating that the order of filling shells 50–82 is not the same for protons and neutrons.

The pairing interaction and related collective effects are apparent in the nature of the first 2^+_1 state in the spectrum of nuclear excited states. Like the mass dependences of the pairing energy, energies $E^*(2^+_1)$ in the isotope and isotone sequences reflect the shell structure of nuclei by showing maxima at magic nucleon numbers [5]. The correspondence between

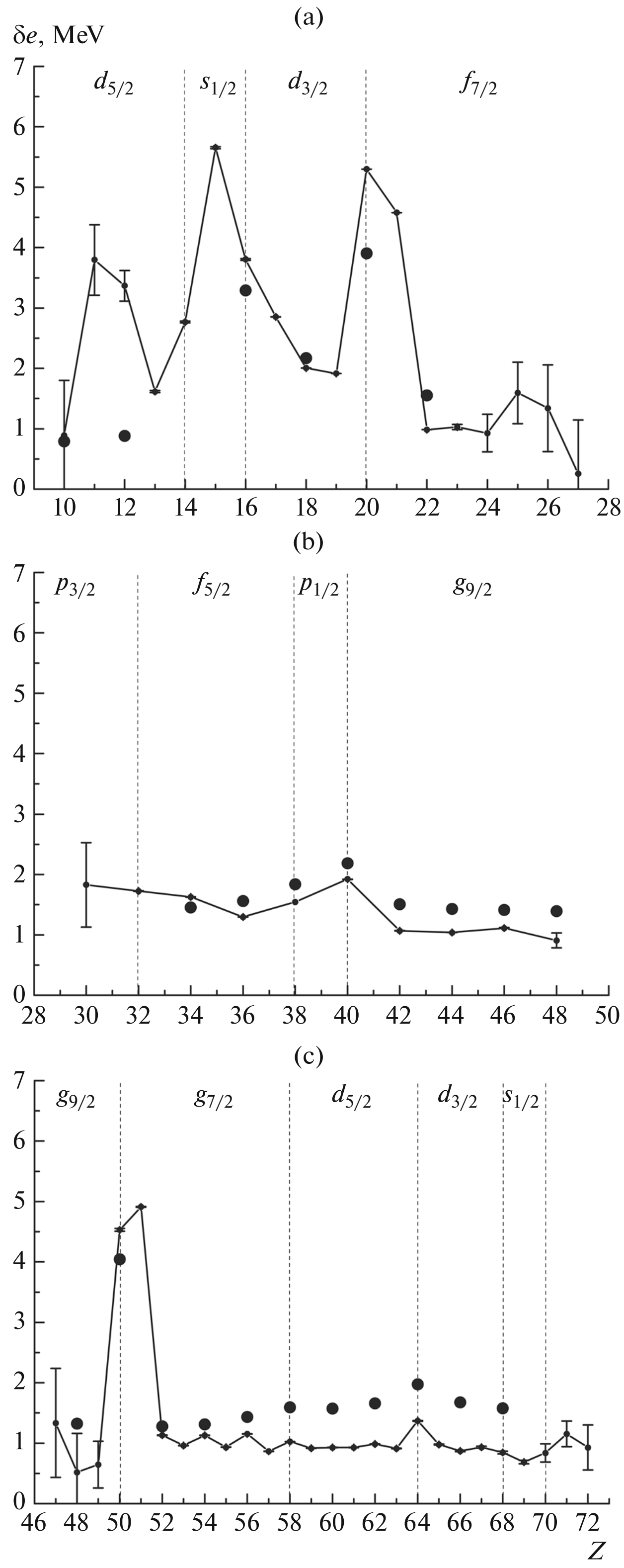

Fig. 5. (●) Excitation energy $E^*(2_1^+)$ [18, 19] and the quantity δe (solid line) as functions of Z for the isotones with N = (a) 20, (b) 50, and (c) 82.

energies $E^*(2_1^+)$ and the magnitude of EOS effect $\Delta_n^{(3)}(N)$ for even–even nuclei was discussed in [20, 21]. This correspondence is exemplified by the emergence of an energy gap in the spectra of tin isotopes. The above characteristics correlate in the chains of magic isotope nuclei for which neutron pairing and shell effects are strongly pronounced. The pattern is less pronounced for nuclei with external proton pairs; in this case, it is the difference between $\Delta_{pp}(Z)$ and $\Delta_{pp}^{(3)}(Z)$ that best reproduces the $E^*(2_1^+)$ behavior both qualitatively and quantitatively. For isotone chains with $N = 20$, 50, and 82, the δe values obtained with formula (10) and those of energy $E^*(2_1^+)$ are shown in Fig. 5.

For $N = 20$ isotones, quantity δe varies strongly with Z, since it largely reflects the shell structure at low j values and with consecutive subshell filling. Only in region Z > 22, where the $f_{7/2}$ shell is filled, does δe reflect the pairing parameter, reaching a constant value of ~1 MeV. In isotone sequences with $N = 50$ and 82, δe behaves more regularly and has an almost constant value of ~ 1 MeV. As in tin isotopes with increasing numbers of neutrons, the subshells in these isotone chains are filled in parallel. In other words, the process can be viewed as the filling of a shell with a net angular momentum of $j = \sum j_k$ where summmation is performed over the corresponding subshells. Note, however, that the $\delta e(Z)$ dependence for $N = 50$ shows a maximum at $Z = 40$, where the filling of the $1g_{9/2}$ subshell begins, and that its 2-MeV fluctuation corresponds to a similar $E^*(2_1^+)$ variation. Similar effects are observed in the $\delta e(Z)$ dependence for $N = 82$, where the there is closure of a subshell group for protons at $Z = 64$. On the whole, $\delta e(Z)$ better reflects such features of the nuclear shell structure as the processes of subshell filling and transitions between the filled and opening subshells.

CONCLUSIONS

The even–odd effect for a nuclear mass surface was formulated in terms of several variables based on nuclear-mass differences and energies of proton separation. Using the isotones of magic nuclei with $N = 20$, 50, and 82 as an example, we showed the even–odd effect is of a complex nature and is induced by nucleon pairing, such multiparticle phenomena as the occupancy of nuclear shells and subshells, and the effects of symmetry. The Z-dependences of the pairing characteristics include the energies of proton separation for two neighboring isotones, $\Delta_{pp}(Z)$ and $\Delta_{pp}^{(3)}(Z)$, are strongly affected by the properties of external nucleons, and reflect both the nucleon correlations in partially filled shells and subshell and shell closures across the magic numbers.

The $\Delta_{pp}(Z)$ dependence is regular for even–even nuclei, since this is expressed through the parameters of two isotones with atomic numbers Z and $Z - 1$ and, for even Z, is not affected by the jump in energy resulting from variation of the proton one-particle energy in the transition to the next subshell. The contribution from multiparticle effects to mass-dependent quantities was estimated using calculations based on the Skyrme–Hartree–Fock approach with no nucleon-pairing effects. Pairing energy $\Delta^{(4)}$ calculated in this manner is low in the regions between the magic numbers and displays local jumps at shell closures. The difference between experimental pairing energy $\Delta_{pp}^{(4)}(Z)$ and the one calculated using the SHF approach qualitatively reproduces the variation of the pairing energy of identical nucleons along with their number. This first grows with subshell occupancy and then falls toward its closure.

Nucleon pairing is apparent in the low-lying collective 2^+ states that form energy gaps of 1–2 MeV in the spectra of excited states of even–even nuclei. Using isotone chains with $N = 20$, 50, and 82 as examples, we plotted excitation energy $E^*(2_1^+)$ as a function of Z and showed it is directly correlated with the $\delta e(Z)$ dependence. On the whole, we found the $\delta e(Z)$ dependence reflects the features of nuclear shell structure better than the form of proton-pairing energy $\Delta_{pp}(Z)$. These features include the processes of successive shell filling and transitions between closed and opening shells.

ACKNOWLEDGMENTS

The authors thank D.E. Lanskoi, M.E. Stepanov, and S. V. Sidorov for their helpful consultations and technical assistance.

REFERENCES

1. Mayer, M.G., *Phys. Rev.*, 1949, vol. 75, p. 1969.
2. Haxel, O., Jensen, H.H.D., and Suess, H.E., *Phys. Rev.*, 1949, vol. 75, p. 1766.
3. Eisenberg, J.M., and Greiner, W., *Microscopic Theory of the Nucleus*, Amsterdam: North-Holland, 1976.
4. Ring, P. and Schuck, P., *The Nuclear Many-Body Problem*, Berlin: Springer, 2004, 3rd ed.
5. Bohr, A. and Mottelson, B., *Nuclear Structure*, New York: W.A. Benjamin, 1969, vol. 1.
6. Jensen, A.S., Hansen, P.G., and Jonson, B., *Nucl. Phys. A*, 1984, vol. 431, p. 393.
7. Madland, D.G. and Nix, J.R., *Nucl. Phys. A*, 1988, vol. 476, p. 1.
8. Moller, P. and Nix, J.R., *Nucl. Phys. A*, 1992, vol. 536, p. 20.
9. Duguet, T., Bonche, P., Heenen, P.-H., and Meyer, J., *Phys. Rev. C*, 2001, vol. 65, p. P. 014311.
10. Dobaczewski, J., Magierski, P., Nazarewicz, W., et al., *Phys. Rev. C*, 2001, vol. 63, p. 024308.
11. Preston, M.A., *Physics of the Nucleus*, Reading: Addison-Wesley, 1962.
12. Wang, M., Audi, G., Kondev, F.G., et al., *Chin. Phys. C*, 2016, vol. 41, p. 030003.
13. Talmi, I., *Phys. Rev.*, 1956, vol. 107, p. 326.
14. Talmi, I., *Simple Models of Complex Nuclei*, New York: Harwood Academic, 1993.
15. Chabanat, E., Bonche, P., Haensel, P., et al., *Nucl. Phys. A*, 1997, vol. 627, p. 710.
16. Imasheva, L.T., Ishkhanov, B.S., Sidorov, S.V., Stepanov, M.E., and Tretyakova, T.Yu., *Phys. Part. Nucl.*, 2017, vol. 48, p. 889.
17. Brown, B.A., in *Fifty Years Of Nuclear BCS: Pairing In Finite Systems*, Broglia, R.A. and Zelevinsky, V., Eds., World Scientific, 2013, p. 179.
18. Evaluated Nuclear Structure Data File. https://www.nndc.bnl.gov/ensdf/.
19. Centre for Photonuclear Experiments Data. http://cdfe.sinp.msu.ru/.
20. Brown, B.A., *J. Phys.: Conf. Ser.*, 2015, vol. 580, p. 012016.
21. Ishkhanov, B.S., Sidorov, S.V., Tretyakova, T.Yu., and Vladimirova, E.V., *Chin. Phys. C*, 2017, vol. 41, no. 9, p. 094101.

Translated by A. Asratyan